6-4-2021

A Modular Peel Fixture for Tape Peel Tests on Immovable Substrates

J.A. Gohl

T.C. Thiele-Sardina

M.L. Rencheck

Kendra Erk

C.S. Davis

A Modular Peel Fixture for Tape Peel Tests on Immovable Substrates

J.A. Gohl[a], T.C. Thiele-Sardina[a], M.L. Rencheck[a],

K.A. Erk[a], C.S. Davis[a*]

[a]School of Materials Engineering, Purdue University, West Lafayette, Indiana, 47907 USA

**Corresponding Author: Email address: chelsea@purdue.edu (C.S.D.), Telephone number: (765)-494-9216, Fax number: (765) 494-1204*

Keywords: PSA, Peel Test, Test Methodology, Adhesives

Abstract:

Background: Peel tests are frequently used to perform measurements of adhesive strength for pressure sensitive adhesive (PSA) tapes. Current lab methodologies for 90° peel tests translate the model substrate orthogonally to the peel direction in order to maintain the peel angle, precluding testing from immovable substrates. Objective: It was our objective to develop a peel fixture capable of testing temporary pavement marking (TPM) tapes and other PSA tapes from immovable substrates such as roadways surfaces. Methods: We present a modular peel fixture for conducting peel experiments directly on immovable substrates. The fixture was validated through a series of peel tests on consumer tapes to reproduce the linear width dependence and viscoelastic rate dependence found in traditional peeling setups. To test the capabilities of the fixture, a series of peel tests were conducted with various tapes on controlled surfaces, and a commercial tape on various immovable substrates. Results: We demonstrate the ability of our fixture to reproduce results reported for traditional peel tests from literature. In addition, we were able to conduct peel tests directly on immovable substrates such as the benchtop. Conclusions:

This fixture shows potential for both traditional peeling tests, and for use in in-situ peel experiments from substrates relevant to the end application of the PSA tape.

1. Introduction

Temporary pavement markings (TPMs) are an important safety tool used by road crews during roadway construction projects. Premature failure of these markings creates dangerous conditions for both drivers and construction workers. TPM tapes are pressure sensitive adhesives (PSAs) that frequently fail due to insufficient adhesion to the pavement surface. Peel tests are a common testing technique to determine the adhesive properties of tapes on relatively small, model substrates, but traditional peel test configurations are not feasible for in situ testing from stationary substrates. A new configuration for peel testing of PSA tapes on immovable substrates is reported.

Peel tests are commonly used for semiquantitative adhesion strength measurements of PSA tapes that allow for the relative comparison of peel strength for quality control and product selection.[1–3] The two most common peel tests are the 180º and the 90º peel tests.[4, 5] The 180º peel test is easier to implement because the technique is uniaxial and can be performed on a standard, single axis load frame without requiring additional fixtures to maintain a constant peel angle.[6] However, by peeling the tape at large angles, significant contributions to the work of detachment (W) come from the bending of the tape.[7] The 90º peel test is the most common and preferred testing method for thicker tapes because it reduces contributions from bending, while also minimizing elastic stretching of the peeled tape.[8, 9] However, this method is more difficult to implement due to the required translation of the peel front which is necessary to maintain a 90º peel angle.[1, 7]

The geometry of a 90° peel test is more complicated because the peel front translates orthogonal to the vertical, debonded tape, making it difficult to test on a uniaxial load frame. Common lab scale 90º peel testing equipment overcomes this problem and achieves a constant peel angle by translating the substrate horizontally through a pulley system while applying a

vertical uniaxial force.[10] If a few degrees of error in the peeling angle is considered acceptable, the peel test can be conducted on a stationary substrate through a long string while the load is applied uniaxially.[11] Other setups translate the load cell at a 45° angle relative to the substrate to maintain the 90° peeling angle.[10, 12] These types of setups are convenient for testing PSAs on small, controlled substrates with known surface roughness and energy. However, the first methodology precludes testing on immovable substrates while peel fixtures of the second design are rather large and have a heavy baseplate, preventing testing directly on stationary substrates. Our new design takes inspiration from the 45° load cell translation method while providing the capabilities for peel testing of tapes from immovable substrates like roadways, allowing for the potential of in situ peel measurements.

A peel test uses an energy balance approach to relate the peel force (P) to W (Eq.1),

$$W = \frac{P}{b}(1 - cos\theta) \tag{1}$$

where b is the width of the tape and θ is the peel angle.[7, 13–15] W is comprised of the thermodynamic work of adhesion and energetic losses within the tape due to bending. While W is not a true measurement of the work of adhesion, it has been referred to as the "effective work of adhesion."[16] Using W values, adhesive performance of tapes can be compared.

2. Materials and Methods

For initial testing and validation of the fixture, clean glass slides were used as a "model" or generic substrate while invisible office tape was used as the model tape. To further explore the measurement capabilities of the fixture, the peel response of various commercial tapes (invisible office tape, duct tape, masking tape, transparent tape, and electrical tape) was then determined. To reduce error in the validation testing of our modular peel fixture (MPF), glass substrates were

thoroughly cleaned (see the supplementary information for details) prior to each peel test. Since peel strength is dependent on the manner by which the tape is applied to the substrate,[17] the application procedure was conducted using a rubber blade to apply uniform pressure along the tape length to ensure full contact with the substrate. Samples were at least 15 cm long to ensure proper application to both the substrate and the carriage.

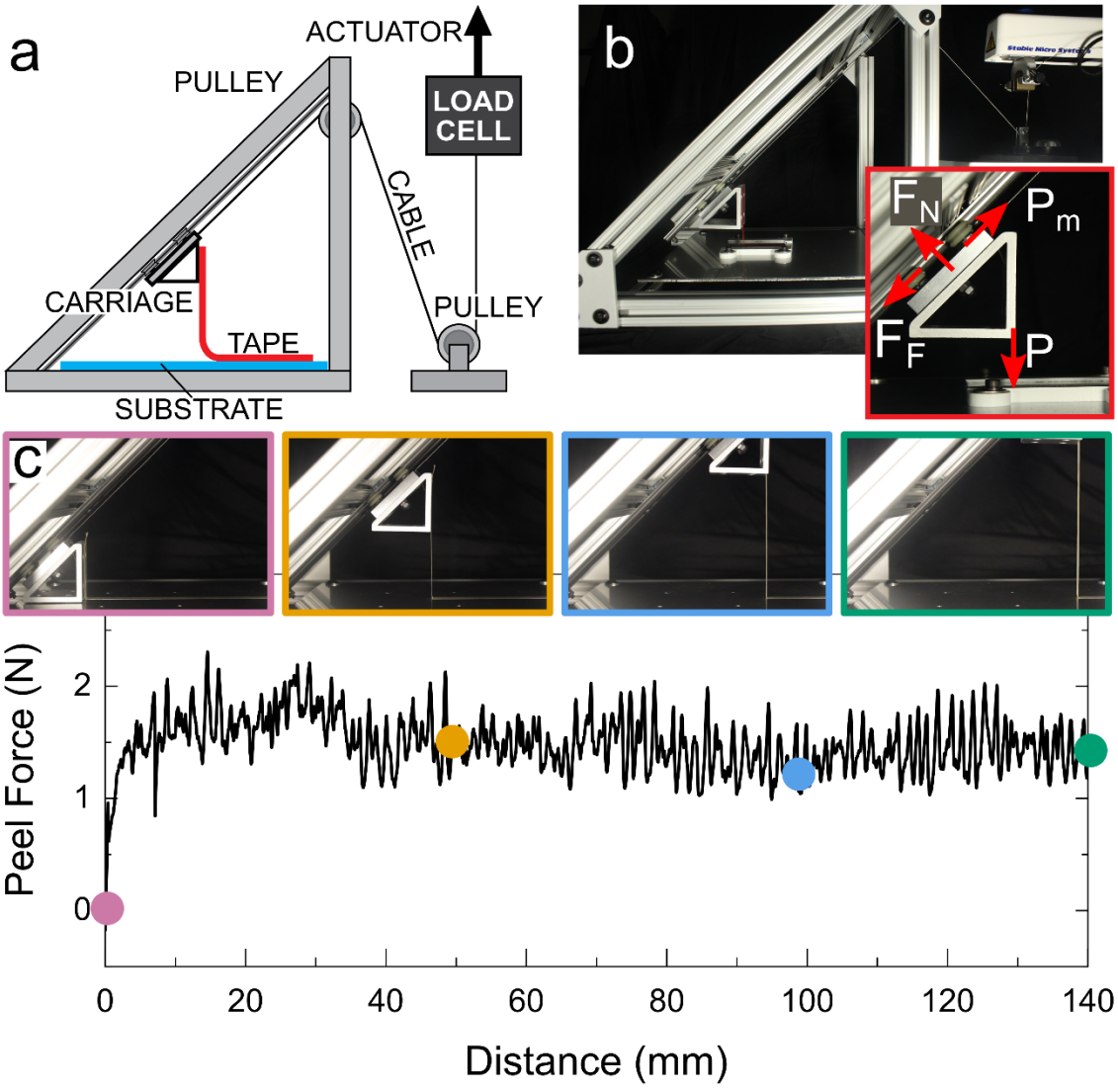

Fig 1 Experimental design of peel fixture. *a)* schematic of fixture *b)* images of the fixture with the inset showing the free body diagram of the carriage. *c)* A representative peel force versus distance plot is included with insets to show the progression of peel.

The design of our MPF utilizes a system of pulleys to translate the carriage at a 45° angle relative to the substrate to maintain the 90° peel angle without moving the substrate (Fig 1a). The peel force of the tape is transmitted through the pulley system and measured by the load cell (Fig 1c), while the vertical displacement is controlled by the load frame.

Due to the geometry of the design (Fig 1b), the measured load (P_m) is not equivalent to the peel force (P) but can be related by Eq.2,

$$P = P_m \left(\frac{\sqrt{2}}{1+\mu_k} \right) \tag{2}$$

where μ_k is the coefficient of friction of the system which was found to be 0.077±0.001 (see supplemental information for further detail). Additionally, the vertical displacement measured by the load frame requires a geometric correction factor of $\frac{1}{\sqrt{2}}$ to determine the true distance travelled by the tape peel front. Using Eq.2, a correction factor of 1.31 was applied to the measured load values to obtain the peel force. All peel force, distance, and rate values presented in this work have been corrected to account for friction, the mass of the harness, and geometry. Data from the first 8mm of peel length have been excluded from all figures, as this region is from pretest portions of the data. At the start of each peel test, there is a spike in peel force corresponding to the higher energy required for crack opening than that required for subsequent propagation of the peel front. For this reason, force measurements from the beginning (first 2mm) of each test were excluded from the analysis. Peel force measurements were averaged over each steady-state peel region.

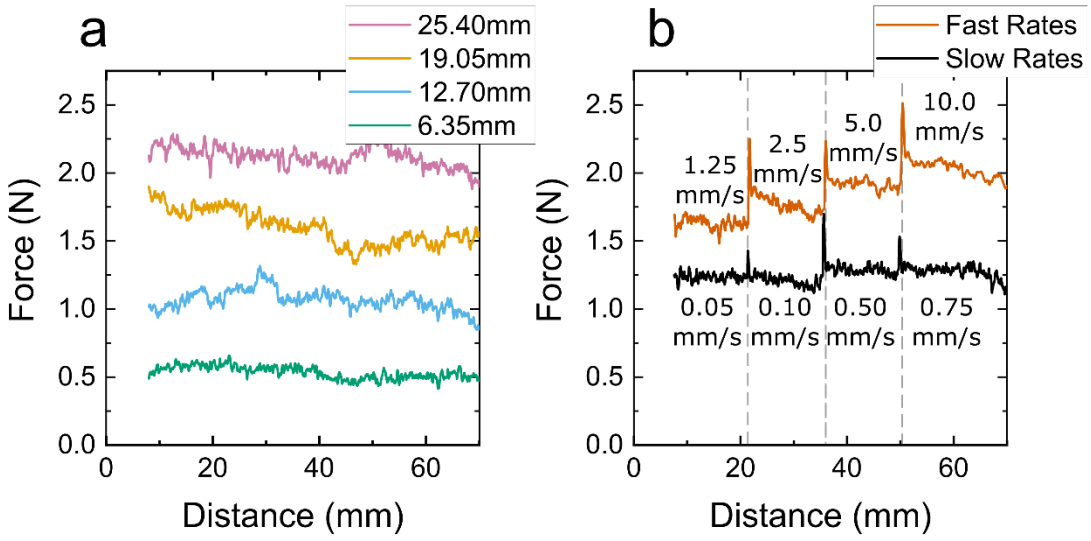

Fig 2 Raw 90° peel force data for invisible office tape on a glass substrate as a function of *a)* tape width and *b)* peel rate.

Invisible office tape was tested over a range of width values (Fig 2a). The peel rate was maintained at 1.25 mm/s while the width of the tape was varied. As expected, the peel force remained constant over each 60 mm long peel experiment and the peel force magnitude increased linearly with increasing width. To further validate the accuracy of the peel fixture, peel rates were varied for the control tape with a constant width of 12.7 mm on the control substrate at rates ranging from 0.05 mm/s to 10.0 mm/s (Fig 2b). Several different rates were applied over the course of a single test following the methodology of Chiche et al., who tested applied different peel rates during a single peel test to increase the throughput of measurements and decrease run to run variation.[18]

3. Results and Discussion

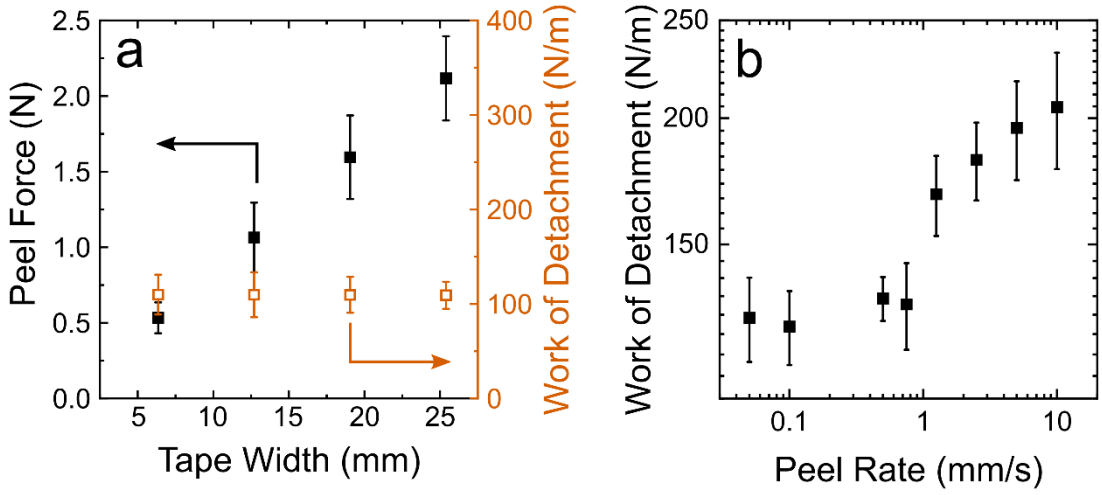

Fig 3 Peel adhesion values for invisible office tape on glass. *a)* The relationship between peel force and work of detachment as a function of tape width at a constant peel rate of 1.25 mm/s. *b)* The relationship between work of detachment and peel rate at a fixed tape width of 12.7 mm. Note that *b)* is on a log-log axis. Each data point is an average of at least 5 samples and error bars represent one standard deviation.

An expected linear relationship between peel force and tape width was observed while maintaining a constant peel rate for our model tape/substrate interface (Fig 3a)[19]. By accounting for the width of the tape, the *W* values calculated by Eq. 1 remained unchanged. While the linear response of peel force and independence of work of detachment as a function of tape width are expected results, testing across a range of widths was necessary to show that the MPF does not introduce any non-linear behavior. It is worth noting that there is a minimum tape width at which this linear trend holds. A non-linear response may be seen in heterogeneous tapes when the width of the tape is of the same order of magnitude as the size of features on the tape.

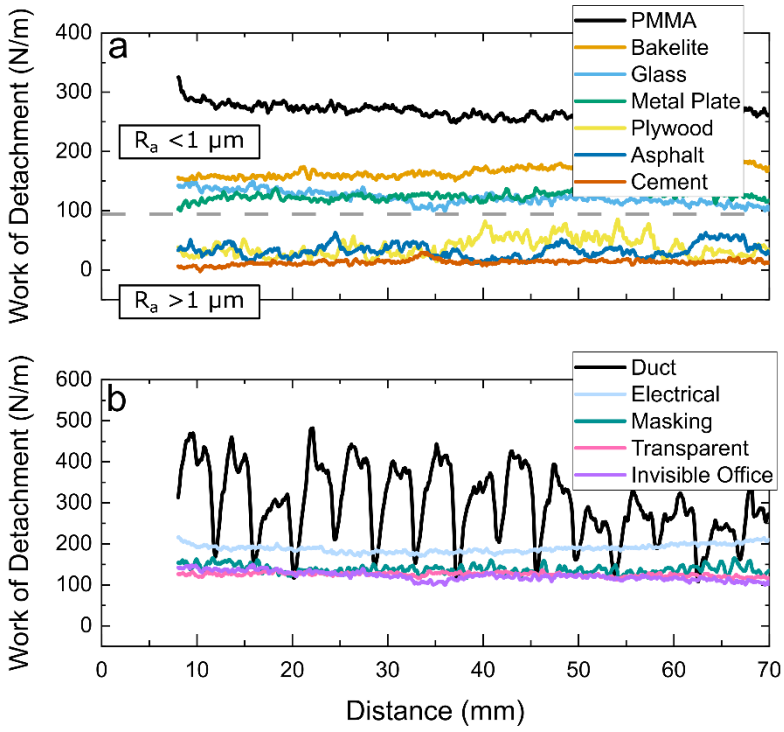

Fig 4 The peel strength varied significantly by substrate and tape. *a)* Work of detachment for transparent office tape on stationary substrates. *b)* Work of detachment for various tapes from stationary glass substrates. All tests were conducted at a peel rate of 1.25 mm/s on tapes of fixed width 12.7 mm

PSA tapes are expected to show a strong peel rate dependence due to their viscoelastic nature.[20–22] For the model tape/substrate, as the peel rate increased, *W* remained constant at relatively low rates and then increased linearly for peel rates higher than approximately 1 mm/s (Fig 3b). This onset of peel rate dependence has been previously reported by Derail et al.[23–25] At low peeling rates, the PSA acts like a liquid and flows, resulting in a low, constant work of detachment. Then, above a critical peeling rate, strain hardening of the PSA occurs, increasing *W*.

To further assess the capabilities of the peel fixture, the peel response of transparent office tape on various substrates and various tapes on a glass substrate were measured (Fig 4). A summary of *W* results of the various tape and substrate can be found in Table 1. The measured work of detachment of the tapes qualitatively follows the expected trends based on intuition and hand feel.

Heavy duty and thicker tapes adhered more strongly to the surface while office and removable tapes had a lower work of detachment.

Table 1: Work of detachment for various tapes and substrates.*

Invisible Office Tape on Various Substrates	
Substrate	**Work of Detachment (N/m)**
PMMA	266±26
Bakelite	168±16
Glass Slides	129±15
Metal Plate	125±18
Plywood	38±21
Asphalt	32±18
Cement	13±16
Various Tapes on Glass Substrate	
Type of Tape	**Work of Detachment (N/m)**
Duct	306±84
Electrical	189±25
Masking	138±32
Invisible Office	129±15
Transparent	125±9

* All tests were conducted at a peel rate of 1.25 mm/s on tapes of fixed width 12.7 mm.

Testing transparent office tape on a variety of different stationary substrates demonstrates the potential of the fixture for peel testing in the field on immovable substrates like roadways. The substrates were selected to include a range of surface energies and roughnesses. Substrates with surface energies more similar to the acrylic adhesive of the tape (e.g. PMMA, Bakelite lab bench) displayed a higher work of detachment than those with dissimilar energies (e.g. metal plate, glass slides). It is important to note that substrates with greater macroscopic surface roughness (R_a roughness >> 1μm) displayed lower work of detachment values than smoother surfaces (R_a

roughness < 1μm) as full contact of the PSA with the surface was not achieved (e.g. asphalt, cement). Representative roughness values can be found in the supplementary information. While the values from this study are only representative, varying the substrates demonstrates the ability of the fixture to differentiate peel forces from substrates other than smooth glass. Additionally, our approach is indifferent to the form factor (size and shape) of the substrate as long as it is planar and has lateral dimensions larger than the width of the tape.

4. Conclusion

Our new design allows for 90° peel testing of PSA tapes from immovable substrates and is capable of obtaining repeatable peel force measurements in good agreement with literature. Additionally, the MPF is sensitive enough to detect the viscoelastic rate dependence of peel force for PSA tapes. The fixture can accurately measure W of various types of tape on a variety of immovable substrates. While this study focused on indoor commercial tapes, the ability to peel from immovable substrates shows potential for deploying the MPF for in situ testing of exterior tapes, as well.

5. Acknowledgements

This work was supported by the Joint Transportation Research Program administered by the Indiana Department of Transportation and Purdue University (Project Number SPR-4423). The contents of this paper reflect the views of the authors, who are responsible for the facts and the accuracy of the data presented herein, and do not necessarily reflect the official views or policies of the sponsoring organizations. These contents do not constitute a standard, specification, or regulation. The authors thank N. Deneke for obtaining optical profilometry measurements and H. Grennan for his contribution to the data analysis.

6. Ethical Statement

The authors declare no conflicting or competing interests.

7. References

1. Zhang L, Wang J (2009) A generalized cohesive zone model of the peel test for pressure-sensitive adhesives. Int J Adhes Adhes 29:217–224. https://doi.org/10.1016/j.ijadhadh.2008.05.002

2. Chen H, Feng X, Huang Y, et al (2013) Experiments and viscoelastic analysis of peel test with patterned strips for applications to transfer printing. J Mech Phys Solids 61:1737–1752. https://doi.org/10.1016/j.jmps.2013.04.001

3. Thouless MD, Yang QD (2008) A parametric study of the peel test. Int J Adhes Adhes 28:176–184. https://doi.org/doi:10.1016/j.ijadhadh.2007.06.006

4. Sugizaki Y, Shiina T, Tanaka Y, Suzuki A (2016) Effects of peel angle on peel force of adhesive tape from soft adherend. J Adhes Sci Technol 30:2637–2654. https://doi.org/10.1080/01694243.2016.1192011

5. Jovanović R, Dubé MA (2004) Emulsion-Based Pressure-Sensitive Adhesives: A Review. J. Macromol. Sci. - Polym. Rev. 44:1–51

6. ASTM D903 - 98(2017) Standard Test Method for Peel or Stripping Strength of Adhesive Bonds

7. Gent AN, Kaang SY (1987) Effect of peel angle upon peel force. J Adhes 24:173–181. https://doi.org/10.1080/00218468708075425

8. Lacombe RH (2005) Adhesion measurement methods: Theory and practice

9. Kendall K (1975) Thin-film peeling-the elastic term. J Phys D Appl Phys 8:1449–1452. https://doi.org/10.1088/0022-3727/8/13/005

10. (2016) ASTM D6862: Standard Test Method for 90 Degree Peel Resistance of Adhesives

11. Peng Z, Wang C, Chen L, Chen S (2014) Peeling behavior of a viscoelastic thin-film on a rigid substrate. Int J Solids Struct 51:4596–4603. https://doi.org/10.1016/j.ijsolstr.2014.10.011

12. Christensen SF, Everland H, Hassager O, Almdal K (1998) Observations of peeling of a polyisobutylene-based pressure-sensitive adhesive. Int J Adhes Adhes 18:131–137. https://doi.org/10.1016/S0143-7496(97)00037-7

13. Kendall K (1973) Peel adhesion of solid films—the surface and bulk effects. J Adhes 5:179–202. https://doi.org/10.1080/00218467308075019

14. Anderson GP, DeVries KL, Williams ML (1976) The peel test in experimental adhesive-fracture mechanics - Paper demonstrates the potential use of peel tests in obtaining adhesive-fracture-energy values. Exp Mech 16:11–15. https://doi.org/10.1007/BF02328915

15. Kendall K (1971) The adhesion and surface energy of elastic solids. J Phys D Appl Phys 4:1186–1195. https://doi.org/10.1088/0022-3727/4/8/320

16. Rivlin RS (1997) The Effective Work of Adhesion. In: Collected Papers of R.S. Rivlin. Springer New York, pp 2611–2614

17. Rezaee M, Tsai LC, Haider MI, et al (2019) Quantitative peel test for thin films/layers based on a coupled parametric and statistical study. Sci Rep 9:1–11. https://doi.org/10.1038/s41598-019-55355-9

18. Chiche A, Zhang W, Stafford CM, Karim A (2005) A new design for high-throughput peel tests: Statistical analysis and example. Meas Sci Technol 16:183–190. https://doi.org/10.1088/0957-0233/16/1/024

19. Gent AN, Schultz J (1972) Effect of Wetting Liquids on the Strength of Adhesion of Viscoelastic Materials. J Adhes 3:281–294. https://doi.org/10.1080/00218467208072199

20. Sun S, Li M, Liu A (2013) A review on mechanical properties of pressure sensitive adhesives. Int J Adhes Adhes 41:98–106. https://doi.org/10.1016/j.ijadhadh.2012.10.011

21. Kovalchick C, Molinari A, Ravichandran G (2014) Rate dependent adhesion energy and nonsteady peeling of inextensible tapes. J Appl Mech Trans ASME 81:041016-1–6. https://doi.org/10.1115/1.4025273

22. Rezaee M, Tsai LC, Haider MI, et al (2019) Quantitative peel test for thin films/layers based on a coupled parametric and statistical study. Sci Rep 9:1–11. https://doi.org/10.1038/s41598-019-55355-9

23. Gibert FX, Allal A, Marin G, Derail C (1999) Effect of the rheological properties of industrial hot-melt and pressure-sensitive adhesives on the peel behavior. J Adhes Sci Technol 13:1029–1044. https://doi.org/10.1163/156856199X00497

24. Marin G, Derail C (2006) Rheology and Adherence of Pressure-Sensitive Adhesives. J Adhes 82:469–485. https://doi.org/10.1080/00218460600713618

25. Derail C, Allal A, Marin G, Tordjeman P (1998) Relationship between viscoelastic and peeling properties of model adhesives. Part 2. The interfacial fracture domains. J Adhes 68:203–228. https://doi.org/10.1080/00218469808029255

Supplementary information for

A Modular Peel Fixture for Tape Peel Tests on Immovable Substrates

J.A. Gohl[a], T.C. Thiele-Sardina[a], M.L. Rencheck[a],

K.A. Erk[a], C.S. Davis[a*]

[a]School of Materials Engineering, Purdue University, West Lafayette, Indiana, 47907 USA

**Corresponding Author: Email address: chelsea@purdue.edu (C.S.D.)*

8. Glass Slide Cleaning Procedure

To ensure variance in testing was from the fixture itself, and not the adhesion between the tapes and glass slides, the glass slides were cleaned through a consistent procedure. As received glass slides were washed with soapy water to remove particulates and polar residues from the manufacturing process. To remove nonpolar residues from the surface, the slides were rinsed with isopropyl alcohol, hexanes, and isopropyl alcohol again. The slides were dried using filtered compressed air after each rinse.

9. Determination of the Coefficient of Friction for the System

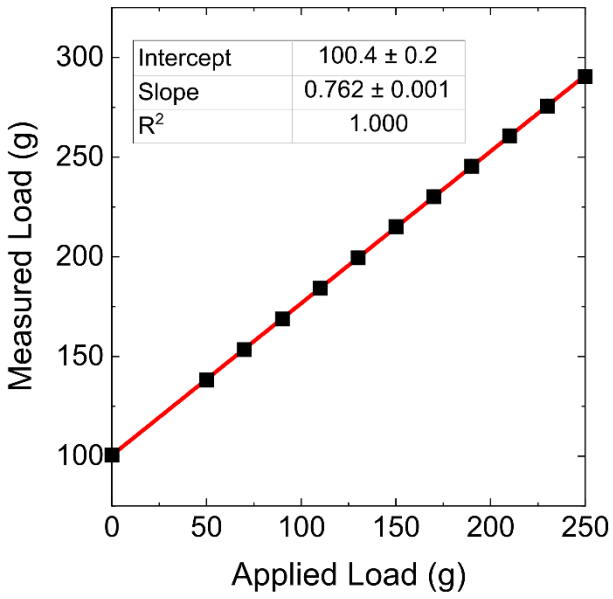

Fig S5 Load measured through the MPF plotted against applied load

To determine the coefficient of friction within the MPF system and to confirm the geometric relationship between the measured load and the peel force, calibrated masses were progressively hung from the carriage. From a free body diagram analysis, it can be shown that the measured load is related to the applied load through Eq. 3:

$$P_m = P_A\left(\frac{1+\mu_k}{\sqrt{2}}\right) \tag{3}$$

where P_m is the measured load and P_A is the applied load and $\mu_k$is the coefficient of friction. From the resulting calibration curve plotting P_m vs P_A , we take a linear fit of the data where the slope of the line is equal to 0.762. ANOVA analysis of this fit determined the standard error of the slope to be 0.001. From equation 3, the slope is equal to $\left(\frac{1+\mu_k}{\sqrt{2}}\right)$ yielding a coefficient of friction of $\mu_k = 0.077 \pm 0.001$.

10.Surface Roughness Characterization

Surface roughness measurements of the glass and PMMA substrates were obtained via optical profilometry (Zygo NewView 8300). The surface roughnesses of the remaining surfaces were obtained from literature. Representative average surface roughness (R_a) values are included below.

Table S2: Representative Surface Roughness

Measured Average Surface Roughness (R_a)		
PMMA	1.361±0.224 nm	
Glass Slides	0.263±0.085 nm	
Reported Average Surface Roughness (R_a)		
Substrate	**Work of Detachment (N/m)**	
Metal Plate	0.1-0.5 µm	[1, 2]
Asphalt	0.1-0.25 mm	[3]
Ground Concrete	12-15 µm	[4]
PMMA	1.5 nm	[5]
Clean Glass	0.9 nm	[6, 7]

11.References:

1. Velling A (2019) Stainless Steel Finishes Explained - DIN & ASTM | Fractory. https://fractory.com/stainless-steel-finishes-din-astm/. Accessed 19 Mar 2021
2. (2014) Roughness measurements of stainless steel surfaces. Euro Inox, Brussels, Belgium
3. Hegmon RR (1979) Definition and measurement of pavement surface roughness. Wear 57:127–136. https://doi.org/10.1016/0043-1648(79)90146-7
4. Garbacz A, Courard L, Kostana K (2006) Characterization of concrete surface roughness and its relation to adhesion in repair systems. Mater Charact 56:281–289. https://doi.org/10.1016/j.matchar.2005.10.014
5. Riau AK, Mondal D, Yam GHF, et al (2015) Surface Modification of PMMA to Improve Adhesion to Corneal Substitutes in a Synthetic Core-Skirt Keratoprosthesis. ACS Appl Mater Interfaces 7:21690–21702. https://doi.org/10.1021/acsami.5b07621
6. Rush MN, Brambilla S, Speckart S, et al (2018) Glass-particle adhesion-force-distribution on clean (laboratory) and contaminated (outdoor) surfaces. J Aerosol Sci 123:231–244.

https://doi.org/10.1016/j.jaerosci.2018.06.002

7. Rasmuson A, Pazmino E, Assemi S, Johnson WP (2017) Contribution of Nano- to Microscale Roughness to Heterogeneity: Closing the Gap between Unfavorable and Favorable Colloid Attachment Conditions. Environ Sci Technol 51:2151–2160. https://doi.org/10.1021/acs.est.6b05911